International Journal on
"Technical and Physical Problems of Engineering"
(IJTPE)
Published by International Organization of IOTPE

ISSN 2077-3528
IJTPE Journal
www.iotpe.com
ijtpe@iotpe.com

December 2020 | Issue 45 | Volume 12 | Number 4 | Pages 19-27

DESIGNING A PD-(1+PI) CONTROLLER FOR LFC OF AN ENTIRELY RENEWABLE MICROGRID USING PSO-TVAC

H. Shayeghi A. Rahnama

Energy Management Research Center, University of Mohaghegh Ardabili, Ardabil, Iran
hshayeghi@gmail.com, alireza.rahnama.001@gmail.com

Abstract- For years, the Load Frequency Control (LFC) of isolated microgrid (MG) has been one of the significant issues in the operation of modern power systems. In this paper, a multistage Proportional Derivative plus (1+ Proportional Integral) (PD-(1+PI)) controller is proposed, to reach the effective regulation of frequency oscillations in an entirely renewable MG with demand response program (DRP). To get the desired level of robust performance, the PD-(1+PI) gains should be optimized. Particle Swarm Optimization with Time-Varying Acceleration Coefficients (TVAC-PSO) algorithm has been used for this aim. Also, a non-commensurable cost function is formulated based on time-domain system characteristics to increase effectiveness of the controller. Besides, to ensure that the taken results are the best ones, various optimization algorithms have been used. The case of the study is a hybrid isolated MG consists of a solar-thermal power plant, micro-hydro, wind, biogas, and a biodiesel generator. The system responses are compared in various operation conditions with PID controller to study the adaptability of the proposed controller. It has a good dynamics response to changes in wind speed, solar irradiation and load in the presence of system nonlinearities and uncertainties. Finally, evaluations show that the proposed control strategy with the support of DRP is superior to the traditional PID controller.

Keywords: Load Frequency Control, Demand Response, PD-(1+PI) Controller, PSO-TVAC, Hybrid Microgrid.

1. INTRODUCTION

1.1. Background

According to the International Energy Agency (IEA) statistics, about 1 billion people around the world, do not access to the electricity network [1]. Various reasons cause this, such as geographical unreachability, economic constraint, and so on. There are two ways to supply electricity to this kind of loads; the first one is the expansion of existing transmission lines, and the second is the establishment of new MGs, which is better to be renewable. Due to some environmental and economic obstacles, the first way is abandoned in recent years. On the other hand, the implementation of a renewable oriented isolated MG is the current trend of solution to this problem.

Over recent years, different small and big power grids blackouts have been reported. For example, on 31 July 2012, about half of India's population suffered the world's most significant power outage. During this blackout more than 620 million people or about 9% of the world population or were affected by it [2].

On the other hand, greenhouse gas (GHG) emissions is a paramount concern. Using renewable energy sources (RESs) can be a great help to reduce environmental pollution due to GHG emissions. RESs based MGs besides the environmental benefits, can be implemented in geographically remote places [2, 3]

In addition to the crucial loads, there can be some supererogatory kinds of loads, such as air conditioners, hybrid electric vehicles (HEVs), clothes dryer, water heaters, and so on. These kinds of loads can contribute to DRPs. In other words, DRP is referred to contributing some available kinds of these non-essential loads in solving the LFC problem by increasing/decreasing their power consumption, which can be a great help to overcome frequency oscillation in MGs [4, 5].

1.2. Literature Review

Various types of controllers and their gains optimization methods have been a trend of research for the last few decades in the power systems [6-9]. For example, robust controller schemes such as sliding mode control (SMC) and second-order SMC were used for automatic LFC task in [10] or mixed H_2/H_∞ method in [11]. However, these strategies are mathematically complicated and hard to understand. Different kinds of traditional controllers, such as the classical integral (I), proportional-integral (PI), proportional derivative (PD), proportional integral derivative (PID), integral minus proportional derivative (IPD) were implemented and evaluated in diverse power systems [8]. Optimizing these classical controller's gains for industrial usages that may meet nonlinearities, higher-order systems, or time delays could be a heavy process. Also, the fuzzy form of these classical controllers has been widely used. But, fuzzy controllers dependency on field expertise for tuning the membership functions and rule base is a non-ignorable point; therefore, an optimization algorithm is the first option to reduce fuzzy system effort and find better fuzzy controller [6, 12-14].

Of course, over recent years, except fuzzy controllers, various kinds of other multistage controllers have been used, such as PI-PD by Saikia et al. [9] or PD-PID by Dash et al. [15] to solve LFC task.

Droop control strategy, which is based on voltage, current, frequency curves, or a combination of them and derived from distributed generation convertors characteristics, is another control strategy in isolated MGs. In [16], a generalized droop control (GDC) scheme have been introduced in order to handle a wide range of load change in the microgrid. Nonlinear droop characteristics were discussed in [17]. Diverse methods are implemented to get the optimum controller gains values. Ziegler-Nichols and Cohen-coon tuning methods are of the famous ways which based on trial and error for tuning classical controller gains; these make the process to have challenging activity [7]. Neural network method has implemented to solve the LFC problem [18], which genuinely needs proper training of the network and causes extending computation time.

There are good achievements about cascade controllers in combination with heuristic optimization approaches in recent studies. PI-PD cascade controller optimized by a modified GWO algorithm with considering plug-in electric vehicles was reported in [19] and PD–PID cascade controller gains optimized with bat algorithm for a multi-area thermal system in [15]. Cascade integral and proportional-derivative (CIPD) controller has been optimized using Moth-flame Optimization for a two-area deregulated power system with hydrothermal generations in each area discussed in [20].

LFC studies using DRPs was discussed in lots of works. In [21] the DRP has been used for a conventional power system. Effects of DRP on peak demand by contributing electric vehicles was discussed in [22]. Pourmousavi et al. implemented the DRP for an isolated hybrid wind-microturbine energy system using Particle Swarm Optimization (PSO) algorithm [23].

1.3. Motivation and Contribution

In this paper, a Proportional Derivative (PD) cascaded with One + Proportional Integral (1+PI) controller is proposed to effective regulation of load-frequency oscillations in a hybrid isolated MG considering DRP. To provide the desired level of system performance considering system uncertainty and nonlinearity, the proposed PD-(1+PI) controller gains should be optimized. Particle Swarm Optimization with Time-Varying Acceleration Coefficients (PSO-TVAC) algorithm [24] has been used for this aim. The PSO-TVAC algorithm has simple concept and high effectiveness with automated time-varying control parameters to obtain global optima solution. Also, a non-commensurable cost function is formulated based on time-domain system characteristics to increase effectiveness of the controller.

The case of study is an isolated solar-thermal power plant, micro-hydro, wind, biogas and biodiesel generator based hybrid MG. The system responses are compared in various operation conditions with PID controller to study the adaptability of the proposed controller. It has a good dynamics response to changes in wind speed, solar irradiation and load in the presence of system nonlinearities and uncertainties. Finally, evaluations show that the proposed control strategy with the support of DRP is superior to the traditional PID controller.

1.4. Outline of This Paper

The rest of this paper is structured as follows: section 2 illustrates the hybrid MG model, and also the plants transfer functions are described in this section. The proposed multistage controller and the optimization algorithm are elucidated in section 3. Results and evaluations are portrayed in section 4, and finally, in section 5, the paper is concluded.

2. MICROGRID CONFIGURATION

2.1. Case of the Study

An islanded MG consisting of five different kinds of RESs is assumed to analyze and show the proposed controller's effectiveness. Just a single controller should control all the plants, as shown in Figure 1. The mathematical model of each component of the system is summarized in this part of the article.

This MG is introduced in [25] and here a new single controller, except two PID controllers is implemented. Besides, 20ms delays in the DRP reaction and also in the input signal of the proposed controller are considered. An aggregated DRP component is integrated into the considered MG.

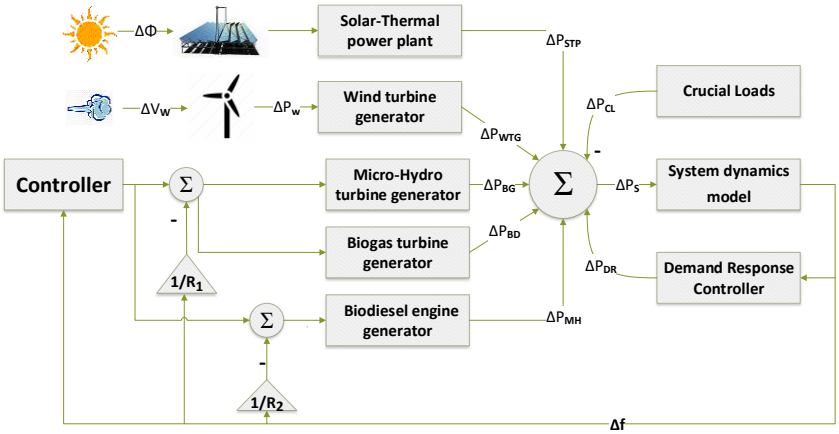

Figure 1. Case of the study

The DRP unit's efficiency is linked to threshold managing accuracy, which is discussed in this section. The numerical value of the symbols is given in Appendix A.

2.2. Wind-Turbine Generator Unit

Here a variation speed wind-turbine with an induction generator is considered as a wind turbine generator (WTG) unit. The radius of blades (R_b) is 23.5m, and the nominal speed (ω_b) is 3.14 rad/s. The generated power is a function of wind speed and estimated as follows:

$$P_W = 0.5\rho C_p A_r V_W^3 \quad (1)$$

where, $\lambda = \frac{R_b \omega_b}{V_W}$; and

$$C_p = (0.44 - 0.0167\beta)\sin(\frac{(\lambda-3)\pi}{15-0.3\beta}) - 0.0184(\lambda-3)\beta.$$

The linearized transfer function of the proposed WTG is introduced as:

$$G_{WTG}(s) = \frac{K_{WT}}{1+sT_{WT}} \quad (2)$$

2.3. Solar-Thermal Power Plant

Equation (3) expresses the transfer function of the Organic Rankine cycle (ORC) based linear Fresnel reflector (LFR) solar-thermal power (STP) plant using thermal oil as heat transfer fluid. It consists of three parts: solar collectors, ORC-based heat-exchanger, and the steam turbine. The approximated linear transfer function model of ORC-based LFR is introduced as:

$$G_{STP}(s) = (\frac{K_{LFR}}{1+sT_{LFR}})(\frac{K_{ORC}\,T_{HX}}{1+sT_{HX}})(\frac{1}{1+sT_{ST}}) \quad (3)$$

2.4. Biogas Turbine Generator Unit

Biogas can replace with traditional diesel generators due to the availability of its fuel (biogas), from biodegradable wastes, including compost and agricultural waste and animal droppings, especially in rural areas. The linearized transfer function of this unit is given by (4).

$$G_{BGTG}(s) = (\frac{1+sX_c}{(1+sY_c)(1+sb_B)})(\frac{1+sT_{CR}}{1+sT_{BG}})(\frac{K_{BG}}{1+sT_{BT}}) \quad (4)$$

2.5. Biodiesel Engine Generator Unit

Biodiesel is a domestic fuel for diesel engines derived from natural oils like soybean oil or extracted from transesterification of other waste edible oils or crops with an appropriate amount of energy. There are two kinds of global biomass-based liquid transportation fuels that might replace gasoline and diesel fuel. These are bioethanol and biodiesel. Unlike the conventional diesel, biodiesel's renewable and less pollution nature has led to renewed interest in the use of vegetable oils to make biodiesel [26].

Equation (5) represents the linearized transfer function of this unit.

$$G_{BDEG}(s) = K_{BD}(\frac{K_{VA}}{1+sT_{VA}})(\frac{K_{BE}}{1+sT_{BE}}) \quad (5)$$

2.6. Micro-Hydro Turbine Generator Unit

Utilizing the potential energy of water and converting it into mechanical energy, in addition to its high efficiency, allows the use of unusable domestic wastewater or even rainwater. The linearized model of micro-hydro turbine generator (MHTG) is approximated as (6).

$$G_{MHTG}(s) = (\frac{K_{MH}}{1+sT_{MG}})(\frac{1+sT_{RS}}{1+sT_{RH}})(\frac{1-sT_{HT}}{1+0.5sT_{HT}}) \quad (6)$$

2.7. Load-Generator Dynamic Model

The aggregate available instantaneous power-changes of the MG can be written as (7) and the frequency deviation in terms of the load-generator dynamics model of the system is estimated as (8).

$$\Delta P_S = \Delta P_{BG} + \Delta P_{MH} + \Delta P_{BD} + \Delta P_{STP} + \\ + \Delta P_{WTG} \pm \Delta P_{DR} - \Delta P_{CL} \quad (7)$$

$$\Delta f = \frac{1}{D+sM}\Delta P_s \quad (8)$$

2.8. DR Unit

Generally, DR appliances that are used for frequency control consist of two main parts: the controller and the electrical appliance. Almost all the DR control methods are based on the frequency deviation (Δf). Consequently, for example, being lower than a specific value of allowable frequency leads to the activation of some amount of DR appliances. A combination of the aggregated DR with a proper frequency threshold management can provide the frequency response's smooth characteristics [21]. Here, the proposed MG contains HEV charging stations as the DRP unit among various DR appliances. Equations (9) and (10), express the linearized model of HEV and the law of the control part of the DRP, respectively. Figure 2 presents the flowchart of the control part of DRP. In this work, the frequency of the MG is 50Hz. Usually, the utility determines the tolerable frequency deviation (Δf_m); in this work, the Δf_m is considered 0.05. Also, the maximum value of DR contribution in frequency regulation will be 20%.

$$G_{HEV}(s) = \frac{K_{HEV}}{1+sT_{HEV}} \quad (9)$$

$$\Delta P_{DR}(s) = \begin{cases} \frac{\Delta f}{|\Delta f_m|}\Delta P_{DRM}, & -\Delta f \le \Delta f \le \Delta f_m \\ \frac{\Delta f}{|\Delta f|}\Delta P_{DRM}, & \text{Otherwise} \end{cases} \quad (10)$$

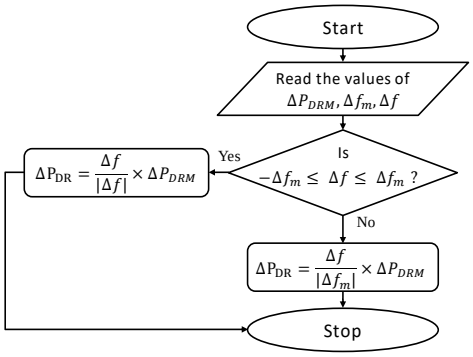

Figure 2. DRP control flowchart

3. PSO-TVAC BASED PD-(1+PI) CONTROLLER DESIGN

3.1. Structure of the Controller

Even though the PID controller has been used broadly in various applications due to its features and simplicity, there are some weak points in this controller's structure. Some of them mentioned briefly in earlier sections. The transfer function of a PID controller for a single area system is defined as (11) [27]:

$$\Delta U = (K_P + \frac{K_I}{s} + s K_D)\Delta f \quad (11)$$

where, ΔU is controlled-error signal and K_P, K_I and K_D are proportional, integral, and derivative gains, respectively. The main functions of each of the terms P, I, and D are described below [7]:

- The proportional term reduces most of the overall error.
- The integral term decreases the final error in a system.
- The derivative term neutralizes the K_P and K_I terms when the output changes quickly, which helps suppressing overshoot and ringing.

The integral controller gains (K_I) must be increased to minimize the steady-state error in the LFC problem, which leads to a lack of performance of the PID controller in transient mode. In fact, it is better to have an inactive or standby an integral part of the controller in transient mode. So, here a Proportional Derivative (PD) cascaded with One + Proportional Integral (1+PI) controller is proposed to handle this issue as well as to effective regulation of load-frequency oscillations in a hybrid isolated MGs with considering DRP and system uncertainty and nonlinearity. As shown in Figure 3, this controller consists of two parts. First, a PD part that works as a filter, and the second part is a PI controller. Thus, it combines these controller's features to enhance the speed of the system's dynamic response by subduing steady-state error and establishing system stability. The transfer function of the proposed cascade controller introduced as (12).

$$\Delta U = (K_P + K_D(\frac{N}{N+s})s)(1 + K_{PP} + \frac{K_I}{s})\Delta f \quad (12)$$

As we can see, in comparison with PID, the proposed multistage controller contains two extra gains. A gain for the controller's filter in the first part and a proportional gain in the second part of the controller. A power system can face with high-frequency noises. The Source of this noise can be radio frequency interference (RFI), such as microwave transmission, radar, arc welding, and distant lightning. These disturbances also can be caused by electromagnetic interference produced by heaters, white goods, and large electrical motors in general [5]. Sometimes, telemetry systems in communication lines cause noises. Using a first-order derivative-based filter in the first stage of this controller structure guarantees to suppress high-frequency noises, which could be generated by sensors in automatic control. The second part of the controller is used to improve steady-state error and establishing system stability.

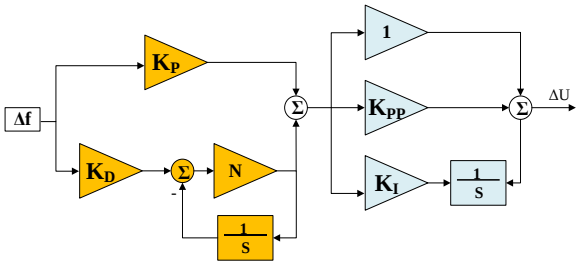

Figure 3. Structure of the proposed PD-(1+PI) controller

3.2. Optimization Algorithm

Designing a proper controller for damping frequency oscillations is a complex optimization problem because there can be multiple local minima and also RESs have some highly intermittent characteristics. Different efforts have been made to reach more effective optimization algorithms. Among the different viewpoints, swarm intelligence, due to its advantages of low parameter setting, fast convergence, robustness, and easy implementation has attracted much attention. PSO algorithm [28] is one of these types of optimization algorithms, which has widely used in the LFC task.

3.2.1. Simple PSO

In the PSO, a specific number of similar individuals, such as members of a flock of birds, a bunch of fishes, or even insects, search for the best way to achieve or to get close to their aims in a limited space. The individual's next move depends on their current velocity, their own best memory, and the best experience of the other group members. So, by adding a new purposefully velocities, particles in the swarm are accelerated to new positions. The above concepts can be formulated as Equation (13).

$$V_i^{k+1} = \omega V_i^k + c_1 \text{rand}_1 \times \left(Pbest_i^k - X_i^k\right) + \\ + c_2 \text{rand}_2 \left(Gbest^k - X_i^k\right) \quad (13)$$

In Equation (13), V_i^{k+1} is the i-th particle's velocity vector in iteration k+1, which indicates how it will move after current iteration. $Pbest_i^k$ refers to the i-th particle's best position and $Gbest^k$ is the global best position, both until the k-th iteration. X_i^k is the position of the particle in iteration k, c_1 and c_2 determine the share of the cognitive component and the communal component, respectively.

Once these are identified, the new position of each member of the group will update as Equation (14).

$$X_i^{k+1} = X_i^k + V_i^{k+1} \quad (14)$$

It is important to moderate the particle's velocity in later iterations to prevent their pendulum behavior around the global optimum. So, there is an inertia parameter (ω) in Equation (13) to provide this. Simply, it can be a constant positive value or a specific value multiple with a random number. However, a descending function of iteration [29] can be a good idea for the value of the ω to solve the stated problem. In Equation (15), a linearly decreasing inertia weight factor is introduced.

$$w = w_{\max} - \frac{w_{\max} - w_{\min}}{\text{iter}_{\max}} \times \text{iter} \quad (15)$$

where, $w_{\max} > w_{\min}$ and $w_{\min} > 0$.

3.2.2. The PSO-TVAC Idea

The normal PSO is usually confined in the local optima in the early iterations and suffers from precipitate convergence when encountering a complex optimization problem. Authors in [24] proposed a kind of PSO that acceleration coefficients change linearly according to the iterations instead of using constant coefficients. They showed that PSO-TVAC could appropriately explore across the search space in earlier stages and converge to the global best in later stages with more confidence.

Clearly, in the initial steps, due to the lack of social experiences, particles in a swarm should act according to their thought. As the particles collect more experience over time (iteration), each particle should use others more [30]. According to this fact, in the PSO-TVAC, c_1 and c_2 are formulated as (16) and (17) for i-th iteration.

$$c_1 = (c_{1f} - c_{1i}) \times (iter / iter_{\max}) + c_{1i} \quad (16)$$

$$c_2 = (c_{2f} - c_{2i}) \times (iter / iter_{\max}) + c_{2i} \quad (17)$$

where, $c_{1f} < c_{1i}$ and $c_{2f} > c_{2i}$.

4. SIMULATION AND THE RESULTS

4.1. Objective Function

Because of its multistage structure and having two more controlling handles, the proposed PD-(1+PI) controller gives more flexibility and adaptability than the conventional controllers. However, this also extends the search space and makes it hard and complicated to find the optimum parameters of the controller. Because of this, the PSO-TVAC algorithm is applied to the optimal tuning of the proposed PD-(1+PI) controller parameters. Consequently, defining a proper objective function (OF) to get the proper results in terms of robustness and speed is necessary. The well-defined OF not only provides desired frequency regulation but also makes it easier for the optimization algorithm to find the global best. In this work, to minimize the frequency oscillations in different scenarios with the penetration of RESs and to use more satisfying of the proposed controller features, the cost function is introduced as Equation (18).

$$OF = w_1.ITAE + w_2.ST + w_3.MOS$$

$$\text{s.t.:} \begin{cases} K_{P_{\min}} \le K_P \le K_{P_{\max}}, \; K_{I_{\min}} \le K_I \le K_{I_{\max}} \\ K_{D_{\min}} \le K_D \le K_{D_{\max}}, \; K_{PP_{\min}} \le K_{PP} \le K_{PP_{\max}} \\ N_{\min} \le N \le N_{\max} \end{cases} \quad (18)$$

$$\text{and} \quad ITAE = \int_0^{t_{sim}} t \, |\Delta f| \, dt$$

where, *ITAE*, *ST*, and *MOS* refer to integral of time-weighted absolute error, settling time, and maximum overshoot, respectively. w_i (i = 1, 2 and 3) are weight factors and K_P, K_I, K_{PP}, K_D, and N are the tunable controller's gain parameters. Choosing a suitable weight factor for each term of the proposed OF could be assigned to an optimization algorithm. Here, we found that w_1=1000, w_2=5, and w_3=1200 are good choices for our purposes. The simulation time (t_{sim}) for finding the optimum controller gains is 3s.

In order to optimal tuning of PID/PD-(1+PI) controller parameters using minimizing the introduced OF, PSO algorithm and spotted Hyena optimizer (SHO) [31], in addition to the PSO-TVAC algorithm, have been applied. For this study, 0 and 10 are taken as the lower and upper bounds of the controller gains, respectively. In the first stage of the proposed controller, N is assumed to be constant and equal to 50. Results of the PID/PD-(1+PI) controller parameters, by applying a 10% step load perturbation where other system parameters (wind and solar) have no variation are listed in Table 1. Convergence curves of the investigated algorithms during 100 iterations have depicted in Figure 4.

Table 1. Optimum parameters of the controllers

	PID Gains			PD-(1+PI) Gains			
	K_P	K_I	K_D	K_P	K_I	K_D	K_{PP}
PSO	5.4493	9.6070	0.1837	3.1400	5.5005	0.7233	0.6677
SHO	1.3946	9.1069	0.2126	2.5425	7.6867	0.2926	1.5361
PSO-TVAC	5.1644	9.6924	0.1493	4.6292	3.8177	1.2233	0.0958

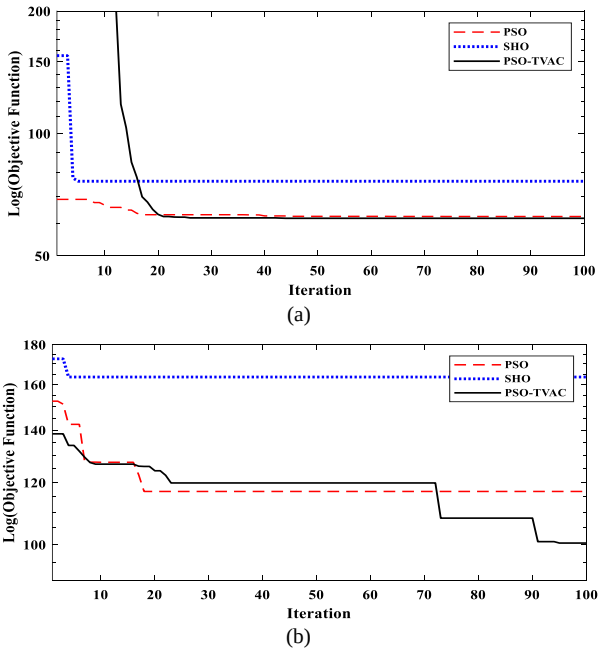

Figure 4. Fitness convergence, (a) PD-(1+PI) and (b) PID; dashed (PSO), dotted (SHO), and solid (PSO-TVAC)

4.2. Evaluations and the Results

In this section, a comparison is being reported for different circumstances of the proposed isolated MG with the PID/PD-(1+PI) controller. Various loading and generating conditions are assumed which are as follows:

- Case 1: Dynamic responses of the system when ΔV_w=0 and $\Delta\Phi$=0

This case analyzes the system's dynamic response to 10% load perturbation where other system parameters (wind and solar) have no variation. This perturbation is applied to the system as a positive step at t=0. Increase the load leads to a frequency drop quickly. The controller and the DRP unit make to settle down the frequency deviations

and provide the system stability just a few seconds after the disturbance, as shown in Figure 5. To illustrate efficiency of the proposed PD-(1+PI) controller some of the important time-domain system characteristics such as settling time (ST), the time integral of absolute error (IAE), the time integral of time-weighted absolute error (ITAE), the time integral of the square error (ISE), and the time integral of time-weighted absolute error (ITSE) are summarized as performance indexes and listed in Table 2.

Also, to better show the advantage of the proposed controller, the improvement percentage of the mentioned indicators by using the proposed control strategy is shown in Figure 6. The improvement percentage of the system characteristics with the proposed controller and using three different optimization algorithms, namely PSO-TVAC, PSO, and SHO are compared and the results are depicted in Figure 7. it is understood that the PSO-TVAC provides better characteristics, so other study cases are evaluated and investigated with this optimization algorithm. It is also clear that the proposed controller can establish the system stability faster than the conventional PID controller.

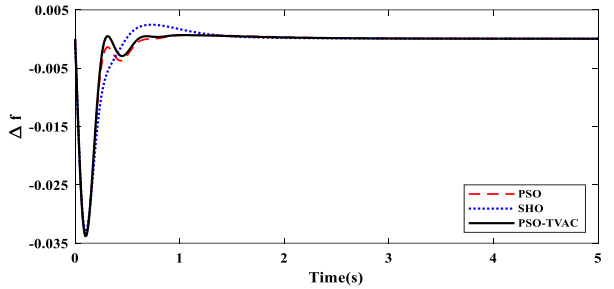

(a)

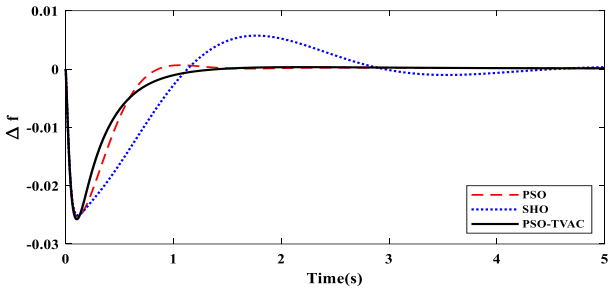

(b)

Figure 5. Dynamic response of the MG to 10% load perturbation with (a) PD-(1+PI) controller, (b) PID controller

Table 2. Time-domain system characteristics of case 1

	Deviation	Optimization Algorithm		
		PSO	SHO	PSO-TVAC
PID	*ST* (s)	1.0891	3.8879	1.1474
	IAE	0.0127	0.0239	0.0125
	ITAE	0.0598	0.0776	0.0590
	ISE ($\times 10^{-4}$)	1.9148	3.0308	1.6632
	ITSE ($\times 10^{-4}$)	0.3666	1.2562	0.3055
	OF	120.7403	163.6080	100.4417
PD-(1+PI)	*ST* (s)	1.075	1.3563	1.055
	IAE	0.0083	0.0093	0.0077
	ITAE	0.0332	0.0399	0.0302
	ISE ($\times 10^{-4}$)	1.3544	1.4579	1.3356
	ITSE ($\times 10^{-4}$)	0.1699	2.0555	0.1623
	OF	62.6784	76.2763	60.8963

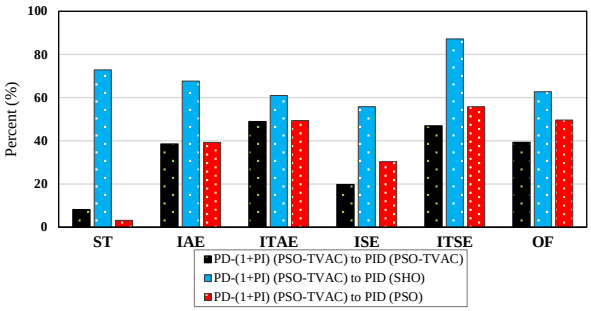

Figure 6. Improvement percentage of the MG's time-domain indexes by using PD-(1+PI) in study case 1

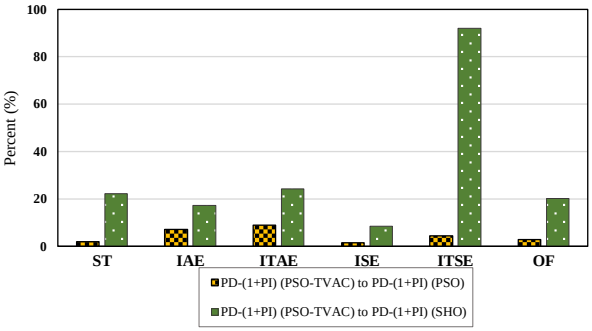

Figure 7. Improvement percentage of the optimized PD-(1+PI) using PSO-TVAC in comparison with PSO and SHO algorithms

• Case 2: After the advantage of the optimized controller with the PSO-TVAC algorithm was ascertained in the previous case, to determine the quality and effectiveness of the DRP, the MG in the presence and absence of the DRP unit with the proposed control strategy is examined in this case. The frequency characteristics of the MG is depicted in Figure 8, and also the system performance indicators are given in Table 3.

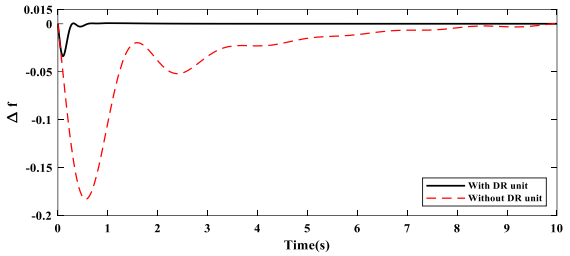

Figure 8. Dynamic response of the MG to 10% load perturbation with proposed control strategy with/without DR unit

Table 3. Time-domain system characteristics of study case 3

	Deviation	
Without DRC	*ST* (s)	9.5869
	IAE	0.4001
	ITAE	6.7316
	ISE ($\times 10^{-4}$)	257
	ITSE ($\times 10^{-4}$)	323
	OF	6782.7
With DRC	*ST* (s)	1.055
	IAE	0.0077
	ITAE	0.0302
	ISE ($\times 10^{-4}$)	1.3356
	ITSE ($\times 10^{-4}$)	0.1623
	OF	60.896

• Case 3: Dynamic response of the MG to monthly average wind speed and solar irradiation during a year

As a more realistic study, the 22-year data of monthly average wind speed and solar irradiation at Bhubaneswar [25] are applied to the MG in 10s time intervals for each month with both PID and PD-(1+PI) controllers in addition to the 10% load increasing at 0s to examine the performance of the proposed control strategy. Figure 9 (a) and (b) show the values of solar irradiation and wind speed during a year, and (c) shows the frequency deviations of the MG. For a better display, the Figure 9(c) is magnified between 20 and 30 seconds. Also, some requisite evaluation indices for this case are presented in Table 4. The results show that the controller performs well in the face of short-term multiple fluctuations and can dampen disturbances faster than the PID controller. This is well reflected in time-dependent indicators.

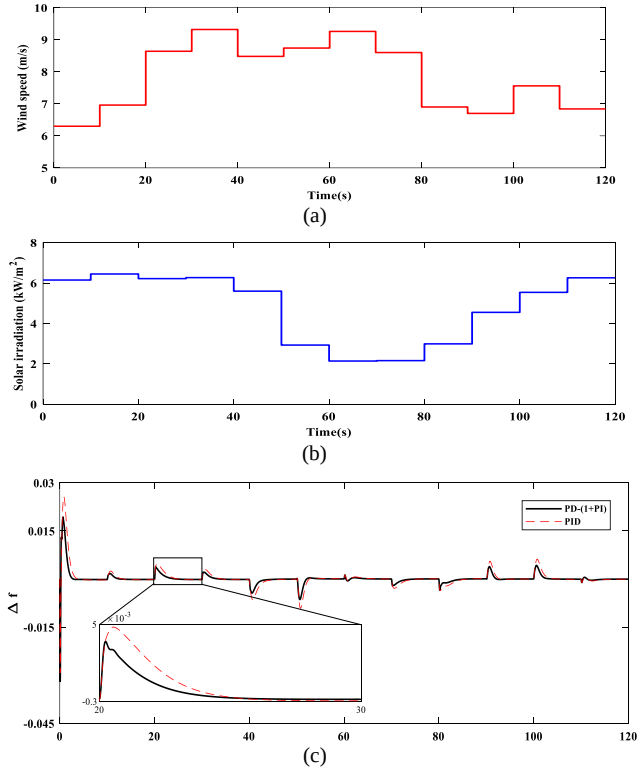

Figure 9. (a) Wind speed (m/s), (b) Solar irradiation (kW/m^2), (c) Frequency deviation of the MG in case 3

Table 4. Time-domain system characteristics of study case 3

	Deviation	
PID	*IAE*	0.1211
	ITAE	4.8345
	ISE (×10^{-4})	9.6600
	ITSE (×10^{-4})	160.89
	OF	5420.34
PD-(1+PI)	*IAE*	0.0686
	ITAE	2.5993
	ISE (×10^{-4})	4.6200
	ITSE (×10^{-4})	57.6400
	OF	3173.97

• Case 4: Dynamic responses of the system for different delay times: Δt_d=20ms, Δt_d=15ms, and Δt_d=10ms

Uncertainties and nonlinearities are crucial issues in the LFC of smart MGs. In the previous cases, it was assumed that there would be a delay of 20 milliseconds in the control signal of the DRP unit and the PID/PD-(1+PI) controller side. Here, in the presence of 10% perturbation in the load side, three different delay periods are considered for the system, and the controller's performances under these conditions are investigated. Figure 10 shows how the delays in control signals affect the system's frequency characteristic with both PID and PD-(1+PI) controllers. It is noteworthy that the controller's parameters are considered as what is obtained by using the PSO-TVAC, and also, the delay times are assumed to be equal for all the control signals. Like previous evaluations, Table 4 is prepared for time-domain indicators. As expected, by reducing the delay in sending/receiving control signals, the system behaves better in terms of the amount of fluctuations i.e., maximum overshoot and undershoot.

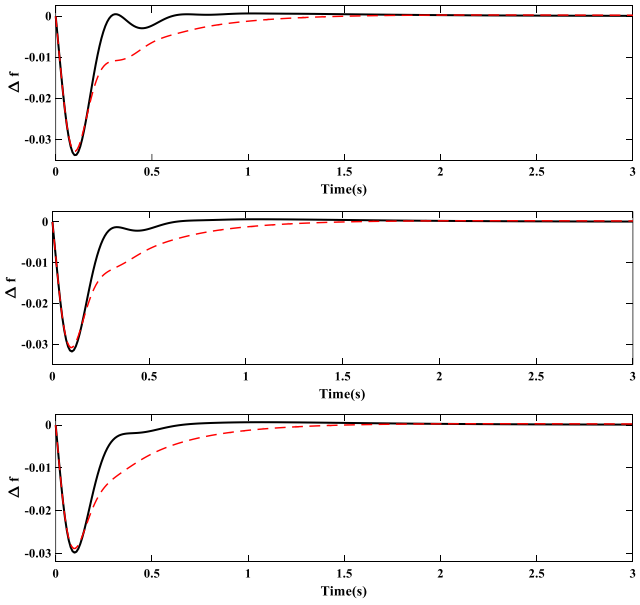

Figure 10. Effects of delays on system's dynamic response, (a) 20 ms, (b) 15 ms and (c) 10 ms delay; solid (PD-(1+PI)) and dashed (PID)

Table 5. Time-domain system characteristics of study case 4

	Deviation	Delay Time		
		10 ms	15 ms	20 ms
PID	*ST* (s)	1.2825	1.2652	1.1474
	IAE	0.0125	0.0125	0.0125
	ITAE	0.0592	0.0591	0.0590
	ISE (×10^{-4})	1.5384	1.5951	1.6632
	ITSE (×10^{-4})	0.3079	0.3058	0.3055
	OF	100.8596	100.4952	100.3765
PD-(1+PI)	*ST* (s)	1.1061	1.0943	1.055
	IAE	0.0076	0.0076	0.0077
	ITAE	0.0303	0.0302	0.0302
	ISE (×10^{-4})	1.1373	1.2234	1.3356
	ITSE (×10^{-4})	0.1434	0.1473	0.1623
	OF	63.1012	62.0921	61.8419

5. CONCLUSION

In this paper, to perform the LFC task for an isolated microgrid, a multi-stage PD-(1+PI) controller is introduced whose parameters are optimized using the PSO-TVAC algorithm. The whole of the load demand in the studied microgrid is supplied by renewable sources, which emphasizes the use of a powerful controller to deal with uncertainty and high fluctuations. Studies conducted throughout the paper show that by using an appropriate objective function, the proposed controller in the presence of the demand response unit shows faster and better performance than the traditional PID controller. The PD-(PI + 1) controller also performs well against consecutive perturbations in a short period of time.

As shown in Figure 6, the proposed controller optimized by the PSO-TVAC algorithm improves the system settling time 28% and reduces the value of the objective function by an average of 60%, compared to the PID controller. Other performance indicators, i.e., ITAE, ITSE, IAE, and ISE, have improved by an average of 53, 63, 48, and 35, in percentage terms, compared to the PID controller, respectively. The superiority of the PSO-TVAC algorithm in optimizing the proposed controller gains over the PSO and SHO algorithms is illustrated in Figure 7. On average, the PSO-TVAC algorithm compared to the SHO and PSO algorithms, improved the indicators by 30% and 5%, respectively.

APPENDICES

1. Values of Symbols

T_{CR}=0.01; T_{BG}=0.23; X_c=0.6; Y_c=1.0; b_B=0.05; T_{BT}=0.2; K_{BG}=0.5; T_{MG}=0.2; T_{RS}=5; T_{RH}=28.75; T_{HT}=1.0; K_{MH}=0.5; R_1=2.0; R_2=2.0; D=0.010; M=0.20; K_{LFR}=5.0; T_{LFR}=0.42; T_{ST}=0.3; K_{ORC}=1; T_{HX}=0.1; K_{WT}=1.0; T_{WT}=1.5; K_{BD}=0.5; K_{VA}=1; T_{VA}=0.05; K_{BE}=1.0; T_{BE}=0.5; K_{HEV}=1.00; T_{HEV}=0.02.

2. PSO-TVAC Parameters

$iter_{\max}$=100; $nPop$=35; c_{1i}=2.5; c_{2i}=0.2; c_{1f}=0.2; c_{2f}=2.5; $w_{\min}$=0.4; $w_{\max}$=0.99.

REFERENCES

[1] L. Bagherzadeh, H. Shahinzadeh, H. Shayeghi, G.B. Gharehpetian, "A Short-Term Energy Management of Microgrids Considering Renewable Energy Resources, Micro- Compressed Air Energy Storage and DRPs", International Journal of Renewable Energy Research, Vol. 9, pp. 1712-1723, 2019.

[2] N. Hatziargyriou, H. Asano, R. Iravani, C. Marnay, "Microgrids", IEEE Power and Energy Magazine, Vol. 5, No. 4, pp. 78-94, 2007.

[3] G. Li, D. Wu, J. Hu, Y. Li, M. S. Hossain, A. Ghoneim, "HELOS: Heterogeneous Load Scheduling for Electric Vehicle-Integrated Microgrids", IEEE Transactions on Vehicular Technology, Vol. 66, No. 7, pp. 5785-5796, 2017.

[4] D. Lee, L. Wang, "Small-Signal Stability Analysis of an Autonomous Hybrid Renewable Energy Power Generation/Energy Storage System Part I: Time-Domain Simulations", IEEE Transactions on Energy Conversion, Vol. 23, No. 1, pp. 311-320, 2008.

[5] N. Kularatna, A.S. Ross, J. Fernando, S. James, "Chapter 1 - Background to Surge Protection", in Design of Transient Protection Systems, N. Kularatna, A.S. Ross, J. Fernando, S. James, Eds.: Elsevier, pp. 1-15, 2019.

[6] P.C. Nayak, U.C. Prusty, R.C. Prusty, A.K. Barisal, "Application of SOS in Fuzzy Based PID Controller for AGC of Multi-area Power System", Technologies for Smart-City Energy Security and Power (ICSESP), pp. 1-6, 2018.

[7] M. Khalilpour, K. Valipour, H. Shayeghi, N. Razmjooy, "Designing a Robust and Adaptive PID Controller for Gas Turbine Connected to the Generator", Research Journal of Applied Sciences, Engineering and Technology, Vol. 5, No. 5, pp. 1543-1551, 2013.

[8] Y.V. Hote, S. Jain, "PID Controller Design for Load Frequency Control: Past, Present and Future Challenges", IFAC-PapersOnLine, Vol. 51, No. 4, pp. 604-609, 2018.

[9] P. Dash, L.C. Saikia, N. Sinha, "Flower Pollination Algorithm Optimized PI-PD Cascade Controller in Automatic Generation Control of a Multi-area Power System", International Journal of Electrical Power & Energy Systems, Vol. 82, pp. 19-28, 2016.

[10] K. Liao, Y. Xu, "A Robust Load Frequency Control Scheme for Power Systems Based on Second-Order Sliding Mode and Extended Disturbance Observer", IEEE Transactions on Industrial Informatics, Vol. 14, No. 7, pp. 3076-3086, 2018.

[11] H. Shayeghi, A. Jalili, H.A. Shayanfar, "A robust mixed H_2/H_∞ based LFC of a deregulated power system including SMES", Energy Conversion and Management, Vol. 49, No. 10, pp. 2656-2668, 2008.

[12] H. Shayeghi, A. Younesi, "A Robust Discrete FuzzyP+FuzzyI+FuzzyD Load Frequency Controller for Multi-Source Power System in Restructuring Environment", Journal of Operation and Automation in Power Engineering, Vol. 5, No. 1, pp. 61-74, 2017.

[13] H. Shayeghi, A. Ghasemi, "Improvement of Frequency Fluctuations in Microgrids Using an Optimized Fuzzy P-PID Controller by Modified Multi Objective Gravitational Search Algorithm", Iranian Journal of Electrical and Electronic Engineering (IJEEE), Vol. 12, No. 4, pp. 241-256, 2016.

[14] H. Shayeghi, H.A. Shayanfar, "Application of PSO for Fuzzy Load Frequency Design with Considering Superconductiong Magnetic Storage", International Journal on Technical and Physical Problems of Engineering (IJTPE), Issue 3, Vol. 2, No. 2, pp. 24-33, June 2010.

[15] P. Dash, L.C. Saikia, N. Sinha, "Automatic Generation Control of Multi-area Thermal System Using Bat Algorithm Optimized PD-PID Cascade Controller", International Journal of Electrical Power & Energy Systems, Vol. 68, pp. 364-372, 2015.

[16] H. Bevrani, S. Shokoohi, "An Intelligent Droop Control for Simultaneous Voltage and Frequency Regulation in Islanded Microgrids", IEEE Transactions on Smart Grid, Vol. 4, No. 3, pp. 1505-1513, 2013.

[17] Y. Sun, W. Huang, G. Wang, W. Wenjun, D. Wang, Z. Li, "Study of Control Strategy of DG Based on Nonlinear Droop Characteristic", in 2012 China International Conference on Electricity Distribution, pp. 1-4, 2012.
[18] F.O. Beaufays, Y. Abdel-Magid, B. Widrow, "Application of Neural Networks to Load-Frequency Control in Power Systems", Neural Networks, Vol. 7, No. 1, pp. 183-194, 1994.
[19] S. Padhy, S. Panda, S. Mahapatra, "A Modified GWO Technique Based Cascade PI-PD Controller for AGC of Power Systems in Presence of Plug in Electric Vehicles", Engineering Science and Technology, an International Journal, Vol. 20, No. 2, pp. 427-442, 2017.
[20] M. Raju, L.C. Saikia, D. Saha, "Automatic Generation Control in Competitive Market Conditions with Moth-Flame Optimization Based Cascade Controller", IEEE Region 10 Conference (TENCON), pp. 734-738, 2016.
[21] Y. Bao, Y. Li, Y. Hong, B. Wang, "Design of a Hybrid Hierarchical Demand Response Control Scheme for the Frequency Control", IET Generation, Transmission & Distribution, Vol. 9, No. 15, pp. 2303-2310, 2015.
[22] S.G. Liasi, M.A. Golkar, "Electric Vehicles Connection to Microgrid Effects on Peak Demand with and without Demand Response", Iranian Conference on Electrical Engineering (ICEE), pp. 1272-1277, 2017.
[23] S.A. Pourmousavi, M.H. Nehrir, C.M. Colson, C. Wang, "Real-Time Energy Management of a Stand-Alone Hybrid Wind-Microturbine Energy System Using Particle Swarm Optimization", IEEE Transactions on Sustainable Energy, Vol. 1, No. 3, pp. 193-201, 2010.
[24] A. Ratnaweera, S.K. Halgamuge, H.C. Watson, "Self-Organizing Hierarchical Particle Swarm Optimizer with Time-Varying Acceleration Coefficients", IEEE Transactions on Evolutionary Computation, Vol. 8, No. 3, pp. 240-255, 2004.
[25] A.K. Barik, D.C. Das, "Proficient Load-Frequency Regulation of Demand Response Supported Bio-Renewable Cogeneration Based Hybrid Microgrids with Quasi-Oppositional Selfish-Herd Optimisation", IET Generation, Transmission & Distribution, Vol. 13, No. 13, pp. 2889-2898, 2019.
[26] A. Demirbas, "Biodiesel, A Realistic Fuel Alternative for Diesel Engines", Springer, London, p. 208, 2008.
[27] P. Kundur, Power System Stability and Control. Palo Alto, California: McGraw-Hill, Inc, 1994.
[28] J. Kennedy, R. Eberhart, Y. Shi, "Swarm Intelligence", Morgan Kaufmann Publishers, San Francisco, 2001.
[29] A. Safari, H. Shayeghi, "Iteration Particle Swarm Optimization Procedure for Economic Load Dispatch with Generator Constraints", Expert Systems with Applications, Vol. 38, pp. 6043-6048, 2011.
[30] H. Shayeghi, A. Ghasemi, "Application of PSO-TVAC to Improve Low Frequency Oscillation", International Journal on Technical and Physical Problems of Engineering (IJTPE), Issue 8, Vol. 3, No. 9, pp. 36-44, September 2011.
[31] G. Dhiman, V. Kumar, "Spotted Hyena Optimizer: A Novel Bio-Inspired Based Metaheuristic Technique for Engineering Applications", Advances in Engineering Software, Vol. 114, pp. 48-70, 2017.

BIOGRAPHIES

Hossein Shayeghi received the B.S. and M.S.E. degrees in Electrical and Control Engineering in 1996 and 1998, respectively. He received his Ph.D. degree in Electrical Engineering from Iran University of Science and Technology, Tehran, Iran in 2006. Currently, he is a full Professor in Technical Engineering Department of University of Mohaghegh Ardabili, Ardabil, Iran. His research interests are in the application of robust control, artificial intelligence and heuristic optimization methods to power system control design, operation and planning and power system restructuring. He has authored and co-authored of 10 books in Electrical Engineering area all in Farsi, one book and 10 book chapters in international publishers and more than 415 papers in international journals and conference proceedings. Also, he collaborates with several international journals as reviewer boards and works as editorial committee of three international journals. He has served on several other committees and panels in governmental, industrial, and technical conferences. He was selected as distinguished researcher of the University of Mohaghegh Ardabili several times. In 2007, 2010, 2012 and 2017 he was also elected as distinguished researcher in engineering field in Ardabil province of Iran. Furthermore, he has been included in the Thomson Reuters' list of the top one percent of most-cited technical Engineering scientists in 2015 -2019, respectively. Also, he is a member of Iranian Association of Electrical and Electronic Engineers (IAEEE) and Senior member of IEEE.

Alireza Rahnama received his B.Sc. degree in Electrical Engineering from Shahid Rajaei Teacher Training University (SRTTU), Tehran, Iran, in 2018 and now he is the M.Sc. student in power systems at University of Mohaghegh Ardabili (UMA), Ardabil, Iran. His research interests are power system control and operation, and applications of heuristic techniques in power systems.